

**Bachelor Thesis**

# **Reconstruction of high-energy neutrino-induced showers in KM3NeT**

Gerrit Zijlstra  
October 2011

Supervisor: Prof. H. Löhner  
Daily supervision: Q. Dorosti  
Kernfysisch Versneller Instituut, Rijksuniversiteit Groningen



## Contents

<b>1</b>	<b>Introduction</b>	<b>3</b>
<b>2</b>	<b>Neutrino</b>	<b>4</b>
2.1	Discovery . . . . .	4
2.2	Properties . . . . .	4
2.3	Neutrino production . . . . .	5
2.4	Candidate neutrino sources . . . . .	5
2.5	Detection of neutrinos . . . . .	6
<b>3</b>	<b>KM3NeT</b>	<b>8</b>
3.1	KM3NeT geometry . . . . .	9
3.2	Detection Unit . . . . .	9
3.3	Multi-PMT Optical Module . . . . .	10
<b>4</b>	<b>Simulation in SeaTray</b>	<b>13</b>
4.1	Particle generation . . . . .	13
4.2	Particle propagation . . . . .	13
4.3	Hit construction . . . . .	14
4.4	Alternative particles and light propagation tool . . . . .	14
<b>5</b>	<b>Shower identification</b>	<b>15</b>
5.1	Reconstruction of showers . . . . .	15
5.2	Quality of reconstruction . . . . .	16
<b>6</b>	<b>Results</b>	<b>18</b>
6.1	Simulations of showers in Antares with AMHiC . . . . .	18
6.2	Simulation of showers in KM3NeT with aAMHiC and AGeMOM . . . . .	20
6.3	Reconstruction of showers in KM3NeT . . . . .	21
6.4	M-estimator performance and cut in KM3NeT . . . . .	23

<b>7 Summary</b>	<b>25</b>
<b>References</b>	<b>26</b>
<b>Appendix A</b>	<b>29</b>
<b>Appendix B</b>	<b>31</b>

## 1 Introduction

Every second the Earth is bombarded from all over the galaxy and beyond with Cosmic Rays (CRs), consisting of high-energy charged particles. In 1991, a particle with an energy of approximately  $3 \times 10^{20} \text{ eV}$  was observed at Dugway Proving Ground, Utah [1]. It was probably a proton traveling with almost the speed of light and was called the "Oh-My-God" particle. The existence of such high energy particles led to questions about the origin or "birthplace" of CRs. Currently, there are two different scenarios trying to explain the "birth" of CRs, i.e. top-down and bottom-up scenarios. The top-down models postulate the existence of "X" particles with mass greater than  $10^{12} \text{ GeV}$  and a lifetime of more than  $10^{10}$  years [2]. The decay of such objects can generate particles of the required energy. The bottom-up model [3] assumes that all high-energy particles are accelerated in astrophysical objects, i.e. cosmic accelerators like black holes and gamma ray bursts. Currently, there are many experiments using different cosmic messengers to search for the origin of CRs such as direct measurement of CRs (at the Pierre Auger Observatory [4]), photons (Fermi Telescope [5] and H.E.S.S. [6]) and neutrinos (Antares [7] and IceCube [8]). Since CRs are charged particles, they are deflected from their path due to magnetic fields. Therefore, the direct detection of CRs cannot give us the clear information about their origins. Photons can provide such information, however, they are often absorbed by interstellar matters. Neutrinos are not affected by magnetic fields, because they do not carry charge. They also hardly interact with matter. Therefore, neutrinos have the ability to travel unaffected through space (Figure 1). Thus neutrinos can be the best messengers to study the origin of CRs, i.e. cosmic accelerators. Neutrinos can be detected through their interactions with matter, creating relativistic secondary particles. These relativistic secondary particles emit Cherenkov light when they are traveling faster than light through a dielectric medium with a refraction index greater than that of vacuum.

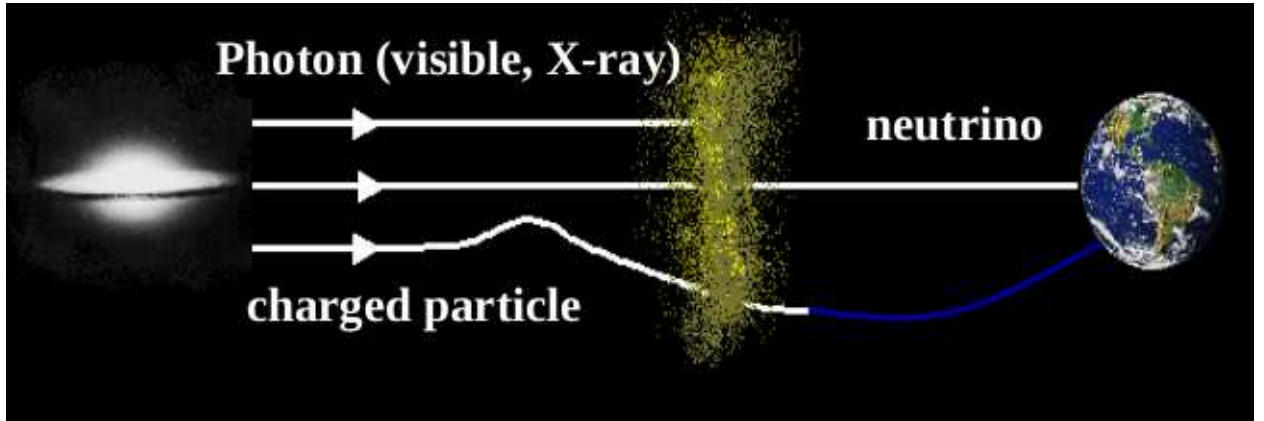


Figure 1: A photon, a charged particle (like a proton) and a neutrino traveling through space. From [9].

## 2 Neutrino

### 2.1 Discovery

The existence of a neutrino was first stated by Wolfgang Pauli in 1930 to explain the energy spectrum of beta-decay. He wrote in his journal [10]:

"I have done something very bad today by proposing a particle that cannot be detected; it is something no theorist should ever do."

**Wolfgang Pauli**

Pauli originally called "his" particle a neutron. Enrico Fermi renamed it in 1931 to neutrino (Italian for small neutral one). In 1934 Fermi developed a theory [11] of beta decay to include the neutrino. This theory presumed the neutrino to be massless as well as chargeless and treated beta decay as a transition that depends upon the strength of the coupling between the initial and final states. The relationship is now known as Fermi's Golden Rule. In 1956, Clyde L. Cowan et al. proved [12] the existence of neutrinos, for which they were awarded the Nobel Prize in 1995. They used a nuclear reactor in which they believed a neutrino flux was produced. This beam was fired upon a tank of water, where the neutrinos interacted with protons to neutrons and positrons. The positrons then would create gamma rays, which were measured. This was the proof for the electron-neutrino,  $\nu_e$ . In the search for other flavors, Leon Lederman, Melvin Schwartz and Jack Steinberger found the muon-neutrino,  $\nu_\mu$ , in 1962. They produced a beam of energetic protons in the Alternating Gradient Synchrotron [13]. With the protons, a shower of mesons ( $\pi$ ) was created and fired on a steel wall made of battleship plates. The mesons decayed into muons and neutrinos, where only the neutrinos were able to pass through the whole wall and ended up into a spark chamber. There, the impact of neutrinos on the aluminum plates produced muon spark trails that could be detected and photographed. This proof of the existence of muon-neutrinos gained them the Nobel prize in 1988. In 1997, 35 years after the detection of the muon-neutrino,  $\nu_\mu$ , direct evidence for the tau-neutrino,  $\nu_\tau$ , was found by the DONUT collaboration [14]. An intense neutrino beam, produced in Fermilab's Tevatron accelerator, which was expected to contain tau-neutrinos, was fired on a sandwich of iron plates and emulsion. A few tau-neutrinos interacted with iron nuclei and produced tau leptons. Tracks, made by the tau leptons ( $\tau$ ) in the emulsion, were photographed proving the existence of tau-neutrinos.

### 2.2 Properties

The neutrino (denoted by  $\nu$ ) is a lepton with a small, non-zero mass. Neutrinos can travel large distances through space in a straight line, because they do not carry charge and therefore are not affected by (inter-)galactic magnetic fields. They are only affected by the weak sub-atomic force, so they can also travel large distances through matter without interaction. Neutrinos are believed to travel with the speed of light, although the results of recent experiments [15] could indicate that neutrinos travel slightly faster than the speed of light.

### 2.3 Neutrino production

In the bottom-up model, neutrino production is believed to be the result of interactions of protons with photons at accelerating astrophysical objects [16]:

$$p + \gamma \rightarrow p + \pi^0 \quad \text{or} \quad (1)$$

$$\rightarrow n + \pi^+,$$

and by  $pp$  and  $pn$  collisions also  $\pi^+$ ,  $\pi^-$  and  $\pi^0$  can be produced. The pions have a short lifetime and decay into neutrinos:

$$\pi^+ \rightarrow \mu^+ + \nu_\mu \rightarrow e^+ + \nu_e + \nu_\mu + \bar{\nu}_\mu; \quad (2)$$

$$\pi^- \rightarrow \mu^- + \bar{\nu}_\mu \rightarrow e^- + \bar{\nu}_e + \nu_\mu + \bar{\nu}_\mu, \quad (3)$$

where  $\bar{\nu}_\mu$  is the anti-particle of  $\nu_\mu$ , and the  $\pi^0$  decays into a pair of photons. There are three kinds of neutrino "flavors": the electron-neutrino  $\nu_e$ , the muon-neutrino  $\nu_\mu$ , and the tau-neutrino  $\nu_\tau$ . The electron- and muon-neutrinos are produced through the reactions shown above, in the ratio  $\nu_e : \nu_\mu : \nu_\tau = 1 : 2 : 0$ . As mentioned in [20], the neutrinos reach a ratio of  $\nu_e : \nu_\mu : \nu_\tau = 1 : 1 : 1$  through oscillations on the way to the Earth. The understanding and determining of the energy dependent flavor composition may lead to new observations or constraints [21] on possible cosmic ray production sites and mechanisms.

### 2.4 Candidate neutrino sources

Possible neutrino producing astrophysical objects, as described by [16] with references to [17–19], are:

#### Active Galactic Nuclei

Active Galactic Nuclei (AGN) are objects at the centre of galaxies which release more non-thermal radiation than other types of objects. The energy for the radiation is thought to be provided by the gravitational energy of matter falling into a super-massive black hole. Sometimes AGNs emit relativistic jets in which neutrinos can be produced. The base for the jets are thermal photons in the accretion disk.

#### Gamma ray bursts

Gamma ray bursts are short, but very luminous eruptions of MeV photons. It is suggested that protons are accelerated in these gamma ray bursts. The accelerated protons and the MeV photons can be the source for mesons like pions, the base for neutrino production.

#### Supernova Remnants

Matter ejected in supernova explosions can collide with interstellar matter. A shock wave at which particles are accelerated, may occur. Cosmic Rays containing these particles can interact with ambient matter, producing pions.

#### Microquasars

Microquasars are like AGNs, but on a much smaller scale. They consist of a central stellar mass black hole or a matter accreting neutron star. Also here, particles are accelerated and interact with photons which lead to the production of neutrinos.

## 2.5 Detection of neutrinos

Neutrinos are uncharged leptons, therefore they are not affected by magnetic fields and they hardly interact with matter. Sometimes a neutrino interacts with a nucleus ( $N$ ), causing a cascade (shower) of hadronic particles. This collision can be a charged current (CC) or a neutral current (NC) interaction with the exchange of charged  $W^\pm$  bosons or the  $Z^0$  boson, respectively. A CC interaction results in the creation of an hadronic shower containing charged particles and a charged lepton as a track-particle (a muon in the case of a  $\nu_\mu$ ). It depends on the neutrino flavor which reaction will take place. Possible CC reactions for the different flavors are:

$$\nu_\mu + N \rightarrow \text{hadronic shower} + \mu; \quad (4)$$

$$\nu_\tau + N \rightarrow \text{hadronic shower} + \tau; \quad (5)$$

$$\nu_e + N \rightarrow \text{hadronic shower} + e. \quad (6)$$

In a NC interaction, the neutrino of any flavor only produces a hadronic shower:

$$\nu + N \rightarrow \text{hadronic shower} + \nu. \quad (7)$$

In a CC interaction the created leptons, besides the shower particles, can on their turn decay or collide. For the tau lepton ( $\tau$ ) and the electron ( $e$ ) these reactions are possible.

$$\tau \rightarrow \nu_\tau + \nu_\mu + \mu; \quad (8)$$

$$\tau \rightarrow \nu_\tau + \nu_e + e; \quad (9)$$

$$\tau + N \rightarrow \nu_\tau + \text{hadronic shower}; \quad (10)$$

$$e + N \rightarrow \text{electromagnetic shower} + X. \quad (11)$$

Combinations of possible reactions (4), (5)+(10), (6)+(11) and (7) are schematically shown in Figure 2.

The electromagnetic shower is produced by an electron losing energy through bremsstrahlung: the electron radiates a photon due to a collision with an other charged particle. This process repeats until the electron has lost most of its energy. In detectors like Antares and KM3NeT the neutrinos cannot be seen directly. However, the relativistic secondaries can be detected as the result of a neutrino interaction in the medium in (or close to) the detector. The presence of neutrinos is noticed by their secondaries through the Cherenkov effect [22]. If a charged particle travels through a medium, atoms along its path are polarized. If the particle travels with a speed less than the speed of light in that medium, the polarized atoms are symmetrically oriented along the particle track. Then the overall dipole moment is zero and no radiation is emitted (Figure 3, left). If the particle travels with a speed greater than the speed of light in that medium, there is no symmetry along the track and radiation is emitted (Figure 3, right) in a "Cherenkov-cone" (Figure 4). The parameter  $\beta = \frac{v_p}{c}$ , with  $v_p$  the speed of the particle and  $c$  the speed of light, defines the angle  $\theta$  of the Cherenkov-cone by:  $\cos \theta = \frac{1}{n\beta}$ , where  $n$  is the refraction index of the medium. Through the reconstruction of photons from the Cherenkov-cone, the direction of the particle track or the location of a shower can be found. The direction of muons can be determined with a much greater certainty than the position of showers, since muons have longer tracks (several kilometers) than shower particles. Muons only lose part of their energy in the detector, making it difficult to determine the energy of the muon. Showers, however, deposit all their energy in a small volume, allowing us to get a better estimate of the energy of the neutrinos producing the shower.



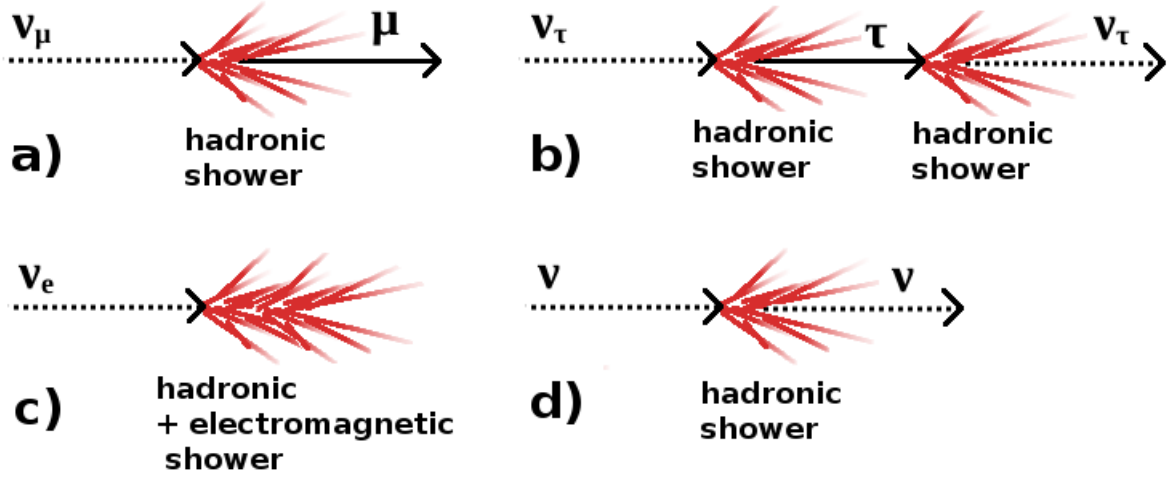


Figure 2: *Schematic view of combinations of possible reactions as described in the text, with a): eq. (4), b): eq. (5)+(10), c): eq. (6)+(11), d): eq. (7).*

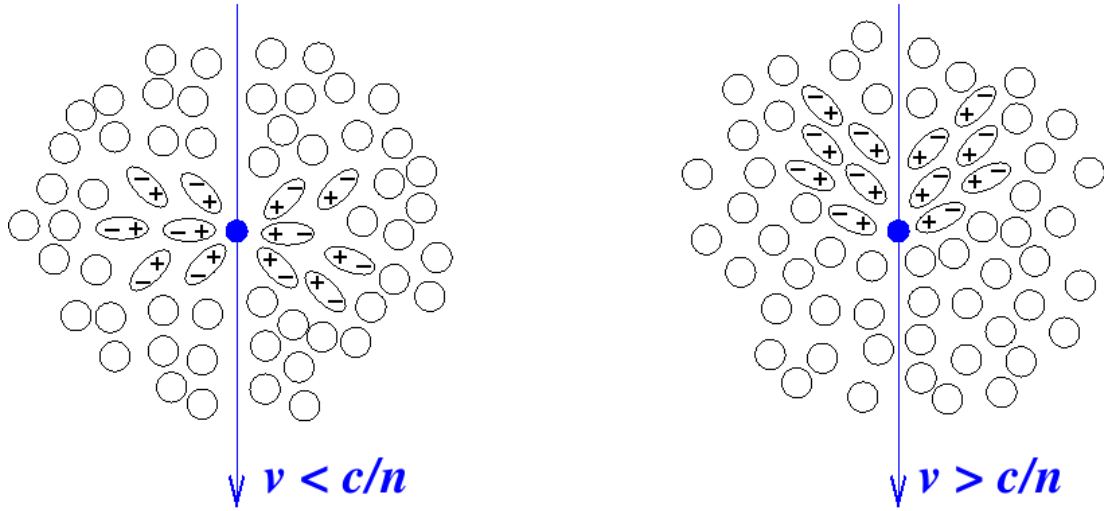


Figure 3: *Schematic view of the production of Cherenkov light in a polarizable medium:  $v$  is the speed of the particle,  $n$  the refraction index of the medium,  $c$  the speed of light. Left: particle traveling with speed  $v < \frac{c}{n}$ . Right: particle traveling with speed  $v > \frac{c}{n}$ . From [23].*

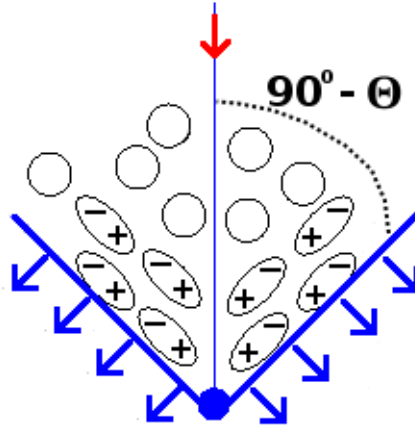


Figure 4: *Geometry of Cherenkov radiation.*

### 3 KM3NeT

KM3NeT is a European research project and the KM3NeT consortium aims to build a multi cubic-kilometers scale neutrino telescope at the bottom of the Mediterranean Sea [24]. It is based on the projects Antares, Nestor [30] and Nemo [31]. Several Detection Units (Figure 5, b)) will form the base of the telescope (Figure 5, a)).

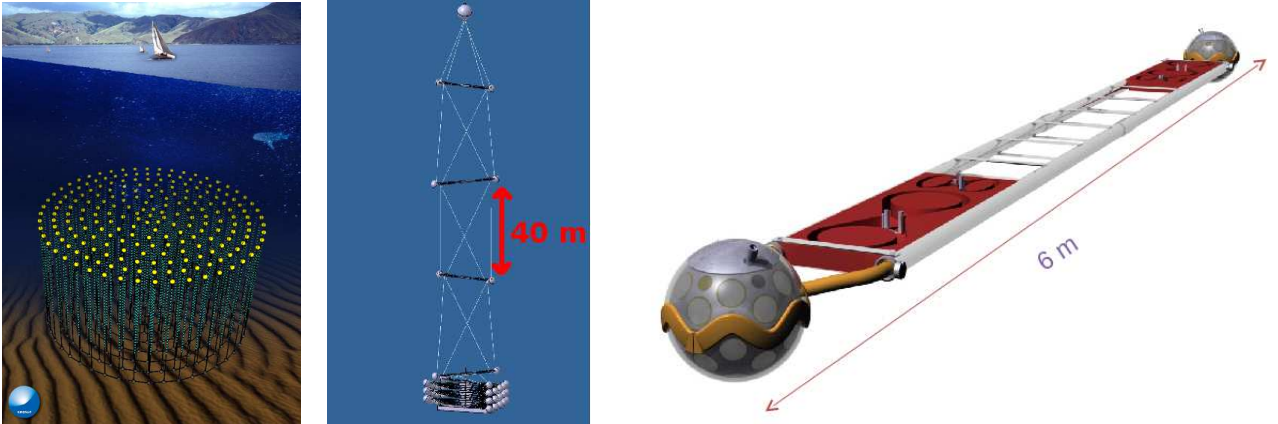


Figure 5: *KM3NeT artist's impression of the (a) telescope, (b) one Detection Unit, (c) one storey with multi-PMT Optical Modules.*

### 3.1 KM3NeT geometry

The final geometrical configurations and the location of the telescope are still not decided. However, the major components, the Detection Units, are defined. The design [25] (11-12-2010) at this moment includes 320 Detection Units. The Detection Units are distributed in a grid-like pattern, shown in Figure 6 (seen from above). The distance between the Detection Units is still under discussion as it depends on the water properties of the final location and will have impact on the quality of the reconstruction methods.

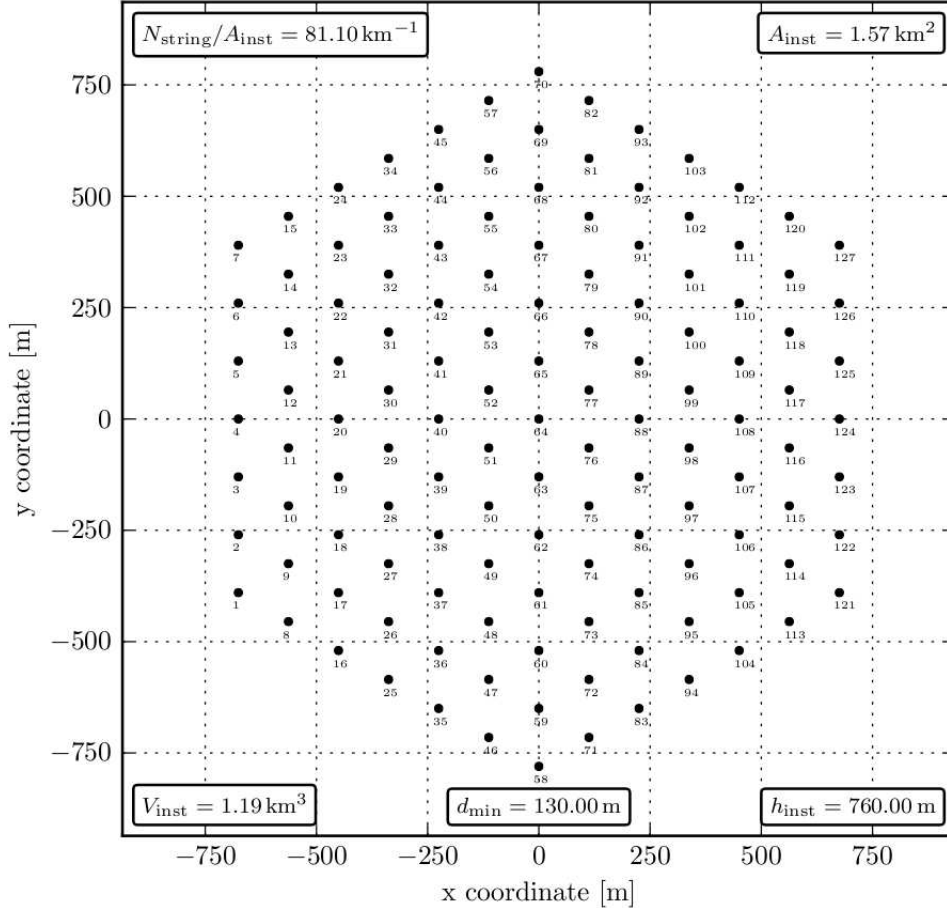


Figure 6: A possible geometrical configuration of KM3NeT with 127 Detection Units, separated by at least 130 meter. The instrumented area is  $1.57 \text{ km}^2$  and with a height of 760 m the instrumented volume comprises  $1.19 \text{ km}^3$ .

### 3.2 Detection Unit

A Detection Unit will be composed of 20 storeys (Figure 5, c)) with a separation distance of 40 meters, making the height of the Detection Unit approximately 900 meters. The storeys are arranged orthogonal to each other in a so-called tower-structure, with the first storey 100 meters above the seabed. While Antares employed per storey a cluster of 3 Optical Modules containing each one large photomultiplier tube (PMT), KM3NeT will use two multi-PMT Optical Modules containing each 31 small PMTs.

### 3.3 Multi-PMT Optical Module

With multi-PMT Optical Modules a large photocathode area, required for the planned sensitivity, can be obtained in a cost effective way. The PMTs that can be used [24] for the Optical Modules are the Hamamatsu R6233-100, with specifications listed in Table 1, and the D783KFLA from ET Enterprises (ETEL). Tests of this ETEL PMT were done at KVI to check the specifications. For the measurements an active voltage divider has been used that leads to a slightly broader anode signal. By shining a laser at different positions of the PMT entrance window, the collected charge (induced by photoelectrons) could be measured as a function of the position. Figure 7 shows this collection efficiency relative to the charge measured at the center of the photocathode, with the used coordinate system depicted in Figure 8. The homogeneous performance justifies the consideration that the whole PMT window-area can be taken as photon sensitive.

Table 1: *Specifications for the Hamamatsu R6233-100 phototube [28].*

Window material	Borosilicate
Photocathode	Super Bialkali
Multiplier structure	Box and Linear focused
Spectral range	300-650 nm
Maximum sensitivity	at 350 nm
Quantum Efficiency at 404 nm	35%

Table 2: *Specifications for the ET Enterprises D783KFLA phototube [29] and KVI results.*

	ET Enterprises	KVI
Quantum Efficiency at 470 nm	20%	
Quantum Efficiency at 404 nm	32%	
Dark Count at 15° C	max. 3 kHz	< 1kHz
Pulse rise time (ns)	2.5	< 2
FWHM (ns)	5	11
Transit Time Spread at the center (ns)	2	< 2.5

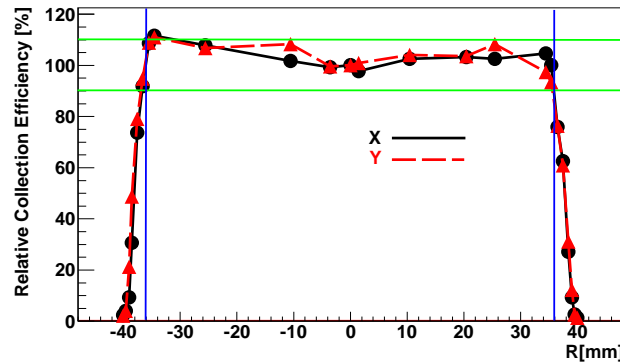


Figure 7: *Relative collection efficiency versus position on the photocathode of the D783KFLA ETEL PMT, normalized to 100% at the centre (radius  $R = 0$ ) of the entrance window. Measurements have been done along the X- and Y-axis (Figure 8).*

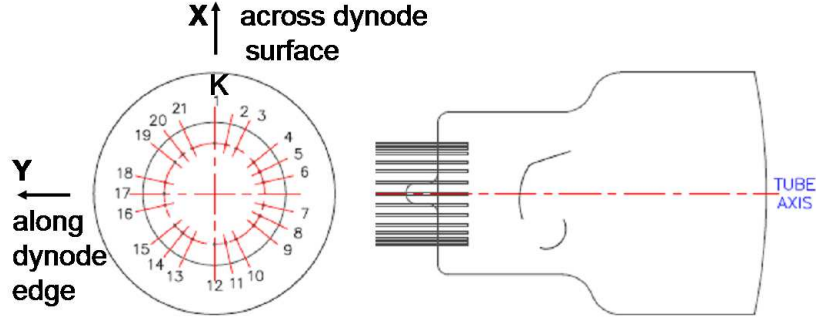


Figure 8: *Coordinate system used for PMT-cathode sensitivity measurements.*

In KM3NeT, each multi-PMT Optical Module (Figure 9, left) will host 31 3-inch PMTs (Figure 9, right) sensitive to single photons. Relativistic secondary and tertiary particles traveling through the detector volume emit Cherenkov light, which will be measured by the PMTs. Even though daylight does not penetrate at a detectable level to depths beyond 1 km, light from the bioluminescence of sea life like *Pyrosoma* (Figure 10) and decay of  $^{40}\text{K}$  causes a continuous optical background. These random background hits are rejected if they cannot be linked through time correlations to an event like a shower or a muon. However, the collision of high-energy protons in the atmosphere creates atmospheric muons which can travel several kilometers during their lifetime and reach the detector to produce additional background signals. To reject them, only up-going events are selected, using the Earth as a natural filter against all particles except neutrinos. With 3-inch- instead of 10-inch-PMTs (used in Antares), the background noise will decrease roughly by a factor  $(\frac{10}{3})^2 = 11$ , making the detection of a photon-pulse from a shower event or muon track more clear.

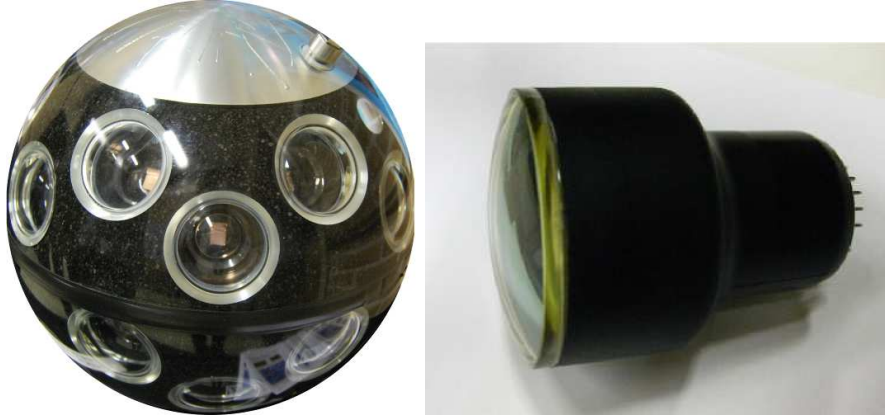


Figure 9: *Left: multi-PMT Optical Module. Right: a single 3-inch diameter photomultiplier tube.*

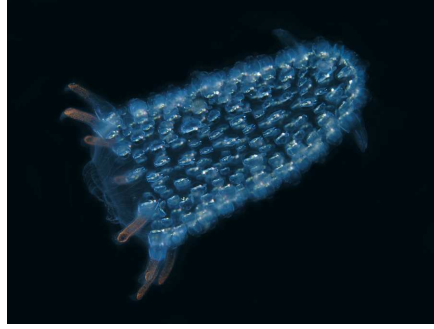


Figure 10: *A Pyrosome with a length of about 1 cm, consisting of hundreds of bioluminescent individuals (zooids) [26].*

## 4 Simulation in SeaTray

With the multi-PMT Optical Module it is possible to detect Cherenkov light emitted from relativistic muon tracks or hadronic showers as the result of the interaction of neutrinos in water. The KM3NeT detector will receive a lot of these signals, together with down-going atmospheric muon background, produced by the interaction of cosmic rays with the atmosphere of the Earth. In order to filter out the requested neutrino signals, a reconstruction and selection strategy has to be applied. By simulating signals, such a method can be developed and tested. In this work, simulations of a neutrino signal in the Antares and KM3NeT telescope are done with two different SeaTray simulation tools. SeaTray is developed from IceTray [27], the software used for the IceCube detector. The basis of SeaTray is the software framework which can be compared to the operating system of a computer. Modules contain algorithms for event reconstruction and simulation act as the "computer programs". The sequence of the modules in the framework is controlled by a C++ code steering file. Data are passed from one module to another in data containers (frames). The framework provides the possibility to attach self-developed modules to the tools.

The neutrino signal simulation is basically divided in three parts: generating neutrinos, propagating created particles, and constructing hits at the detector. The three parts are schematically shown in Figure 11 and discussed in the following subsections. A full description can be found in [35].

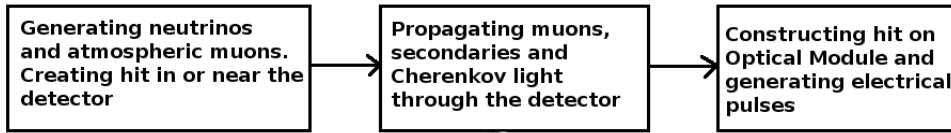


Figure 11: *Block diagram of the simulation steps containing particle generation, propagation and hit construction.*

### 4.1 Particle generation

Incoming neutrinos can be simulated with a neutrino generator called ANIS (All Neutrino Interaction Simulation) [32]. ANIS performs a complete propagation through the Earth, including all neutrino-nucleon interactions. The interactions take place not only inside the detector volume, but also in a surrounding cylinder called the "Can" in order to produce a realistic spread of the interactions. When neutrinos have reached the detector depth, they are forced to interact (Figure 12, left). The result and output of the interaction are the particles given in eqs. (4), (5), (6) and (7). However, neutrino telescopes are so far not able to distinguish between different types of hadronic showers. The hadronic energy is therefore classified in the output stream as a special single particle type. ANIS is able to simulate all three neutrino flavors. Beside the neutrino flavor, other parameters can be adjusted: the neutrino energy ( $E$ ) range (a minimum and maximum energy) and a power-law spectrum (for example  $E^{-2}$ ) for neutrinos.

### 4.2 Particle propagation

The secondary particles generated near the detector have to be propagated to the detector volume. This is done with the Muon Monte Carlo (MMC) propagator, simulating the energy-loss of secondaries when they travel through matter: ionization losses, bremsstrahlung, photo-nuclear interactions and pair production [33]. This tool was originally developed for IceCube and has been recently adapted for

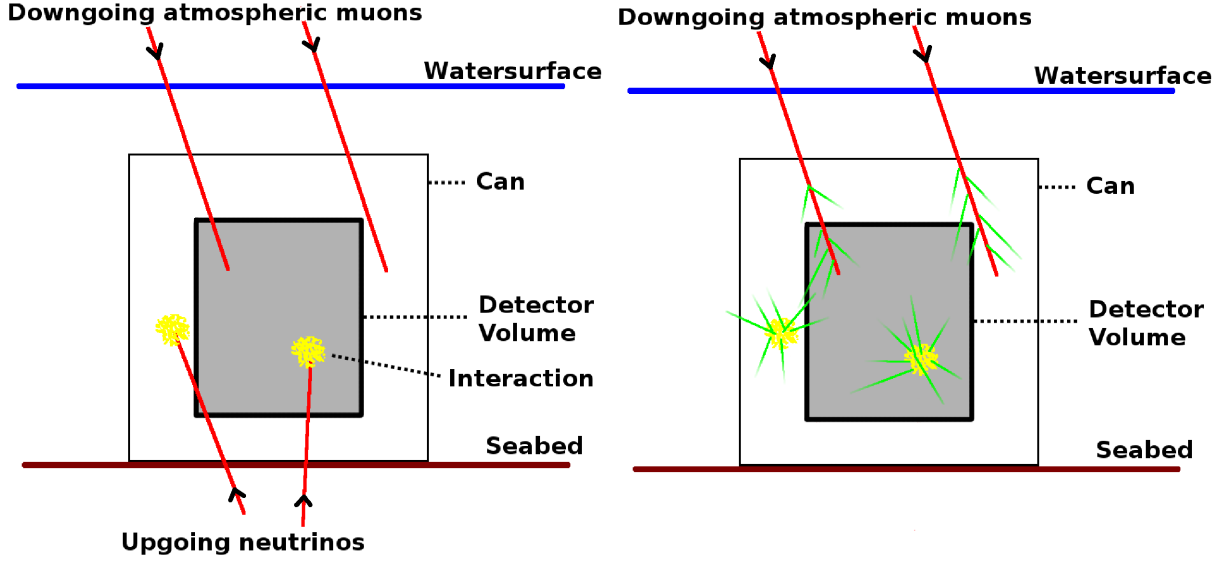


Figure 12: *Left: generation of atmospheric muons, neutrinos and events in the can. Right: propagation of secondaries and Cherenkov light, displayed by the green lines.*

Antares. Here, we call this tool AMHiC (Anis Mmc Hit Constructor). In this work, we developed the AMHiC tool for simulations in KM3NeT.

#### 4.3 Hit construction

Once the photons arrive at the Optical Modules, hits have to be simulated. Photons are propagated through the Optical Module until they are either absorbed or hit the photocathode of one of the individual PMTs (see Figure 13). The photon flux and time distributions at the Optical Modules are parametrized by tables produced by Photonics, a photon tracking package [34]. Photonics needs tables that are specific for the type of water surrounding the detector and contain typical PMT specifications as angular acceptance, Quantum Efficiency and reflectance. This step also includes the conversion of photons into photoelectrons at the photocathode and propagation to the first dynode, which is described by the collection efficiency. These simulated hits need to be converted into measured electrical pulses. Then the pulses have to be evaluated by a trigger algorithm, which decides whether it should be recorded or not.

#### 4.4 Alternative particles and light propagation tool

For KM3NeT, an alternative method for the propagation of secondaries and Cherenkov light has been developed by Claudio Kopper [35]. It also uses the MMC propagator to propagate secondary particles up to the detector volume, but once the secondaries have reached the detector volume, the Geant4 [36] simulator keeps track of them. Secondary particles and their Cherenkov light are propagated through the detector (Figure 12, right). The propagation of light from showers is done by parameterizing the shower approximately as a point-like light source. Some modules from the script that covers the propagation are shown and explained in Appendix A. Considering the geometry of the detector, photons are propagated towards the multi-PMT Optical Modules. This tool we will call AGeMOM (Anis Geant4 Multi-pmt Optical Module).



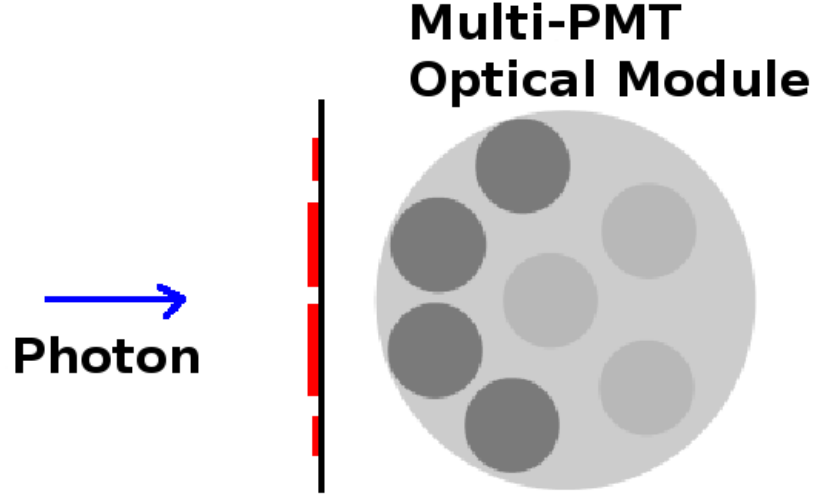


Figure 13: *Projection perpendicular to the photon direction of the photocathode area visible for a photon in the multi-PMT configuration.*

## 5 Shower identification

The numerous down-going (atmospheric) muons create a huge background in which it is hard to identify showers created by neutrinos. A new method to select up-going neutrino-induced showers in Antares has been developed by Qader Dorosti [38]. First, an estimation of the direction of the events is made in order to reject down-going atmospheric muons. If the event is up-going, the position and time of the interaction of the event are reconstructed under the assumption that showers act as point-like sources of light. Suitable discriminating parameters have been defined to evaluate the reconstruction quality. A lower mean value of the distribution of the reconstruction quality parameters is expected for a shower-like event, compared to that for muons. The discriminating cut between the two differentiations is optimized to select shower events with high efficiency and high purity. Purity is defined as the amount of selected showers compared to the pollution of accidentally selected muons. By the use of Monte Carlo simulations, the parameters of the selection strategy were optimized to adapt the strategy for reconstructions on real Antares data. In this work, the method was implemented for the reconstruction of simulated showers in KM3NeT.

### 5.1 Reconstruction of showers

The reconstruction of showers is divided in two steps: a prefit and an M-estimator. The prefit is explained in the following case. If a shower event with space-time position  $\vec{X}_s = (x_s, y_s, z_s, i(c/n)t_s)$  occurs inside a detector, the light of the shower can hit a certain number of PMTs (Figure 14). The PMTs record the space-time coordinates of the hit:  $\vec{X}_i = (x_i, y_i, z_i, i(c/n)t_i)$ , where  $c/n$  is the velocity of light in water with the refraction index of  $n$ . Considering that showers act as point-like sources of light, the time the photons need to reach the PMTs and the distances  $d_i$  of the PMTs from the shower

center should have the relation:

$$\sqrt{(x_s - x_i)^2 + (y_s - y_i)^2 + (z_s - z_i)^2} - \frac{c}{n}(t_i - t_s) = 0, \quad i = 1, 2, \dots, N, \quad (12)$$

where  $N$  is the number of hit PMTs. This set of  $N$  equations can give an analytical solution for the unknowns, using pairwise subtraction of the equations. A residual parameter tells how well the equations are solved, thereby judging how much the shower event looks like a point source of light. For a perfect point source, the residual parameter will be zero. Shower events are expected to appear much more like a point source than muons tracks. Therefore, showers are distinguishable from atmospheric muons.

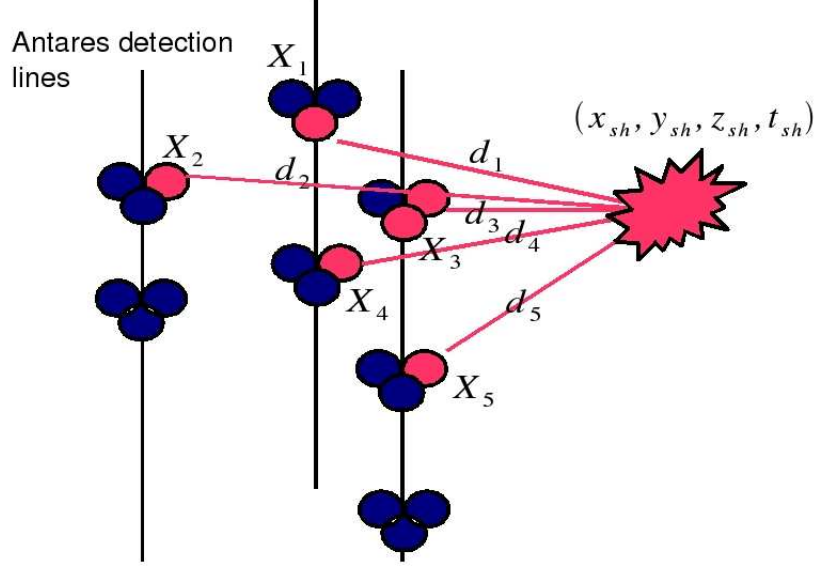


Figure 14: *Light detection from a shower event with space-time position  $\vec{X}_s = (x_s, y_s, z_s, i(c/n)t_s)$ , hitting 5 PMTs (red circles) on Antares detection lines.*

## 5.2 Quality of reconstruction

The reconstruction of the position of the shower can be compared to the true MC position and time. Typical distributions for the position and the timing resolution of the showers are shown in Figure 15. Figure 15 left tells the difference  $\Delta r$  between the (true) Monte Carlo position of the shower  $r_{MC}$  and the reconstructed position  $r_{reco}$ . Figure 15 right shows the equivalent distribution for the time. If  $\Delta r$  and  $\Delta t$  are distributed around 0, as in Figure 15, the reconstructed space-time position of a shower event is almost the same as the true space-time position.

A measure of the quality of the reconstruction is given in the second step by minimizing the M-estimator parameter. A typical distribution is shown in Figure 16. The M-estimator function is based on a  $\chi^2$  function for a hit selection. It minimizes the difference between the measured time  $t_i$  and the expected or theoretical time  $t_{th}$ , with  $t_{th}$  defined as

$$t_{th} = t_s + \frac{n}{c}d_i, \quad (13)$$

and usually has a modification [37] to make the hit selection less sensitive to outliers which cause some fluctuations in the error estimate. Such outliers might be caused by background noise. Then the

M-estimator function becomes:

$$M(t_i, t_{th}) = 2 \times \sqrt{1 + \frac{(t_i - t_{th})^2}{2\sigma_i^2}} - 2, \quad (14)$$

where  $\sigma_i$  represents the error on the measurement of  $t_i$ . Low values of the M-estimator indicate a better reconstructed shower.

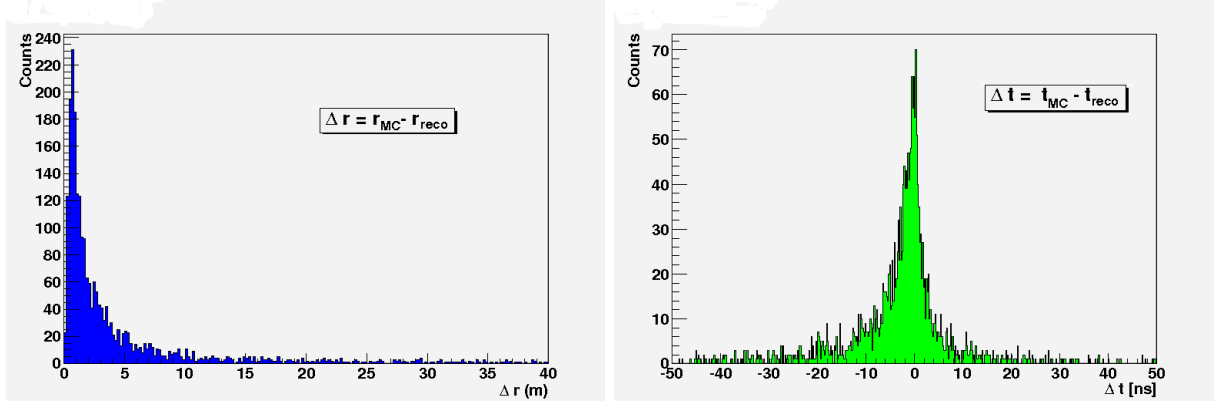


Figure 15: *Typical performance of the reconstruction method for showers, showing the distributions for the position (left) and timing accuracy (right) of the showers.*

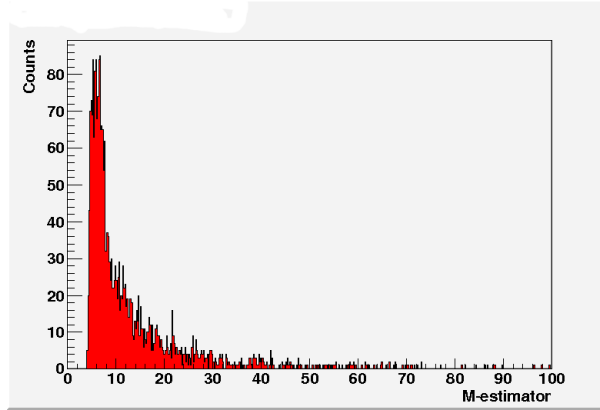


Figure 16: *Typical distribution of the M-estimator quality parameter for showers. In the ideal case, the peak would be distributed around M-estimator 0, i.e. a sharper peak, shifted to the left.*

## 6 Results

The performed simulations with the new selection strategy can be divided in three parts: Simulations of showers in Antares with AMHiC, simulations in KM3NeT with AMHiC and AGeMOM, and reconstruction of showers in KM3NeT. The different simulation tools are described in Section 4.2 and Section 4.4.

### 6.1 Simulations of showers in Antares with AMHiC

The new simulation tool AMHiC has been compared to the standard Antares simulations by analyzing showers. CC  $\nu_e$ -induced hadronic showers, simulated with AMHiC, and NC  $\nu_\mu$ -induced hadronic showers from standard Antares simulations were considered. Figure 17 shows the comparison of the results of the two simulation tools in which the probability density function for  $\Delta t(true)$  is shown.

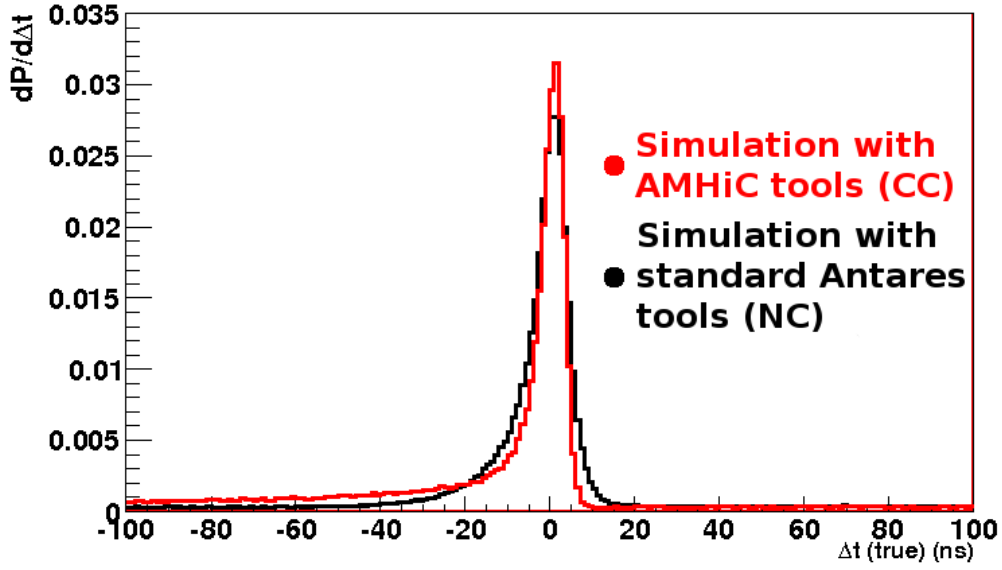


Figure 17: *Probability density functions of the standard Antares simulation tool on  $\nu_\mu$ -induced hadronic showers (black), and the new AMHiC tool on  $\nu_e$ -induced electromagnetic + hadronic showers (red).*

$\Delta t(true)$  is defined as the difference between the measured time of hit  $t_{hit}$  and the expected arrival time of photons which originate from the shower and travel the distance  $D_{MC}$ , shown in Figure 18, from the shower interaction vertex to the hit optical module:

$$D_{MC} = X_{hit} - X_{sh} \quad (15)$$

The expected arrival time can be calculated through

$$t_{expected} = \frac{D_{MC}}{v_{light}}, \quad (16)$$

where  $v_{light}$  is the speed of light in seawater. Therefore,  $\Delta t(true)$  can be defined as:

$$\Delta t(true) = t_{hit} - t_{expected} \quad (17)$$

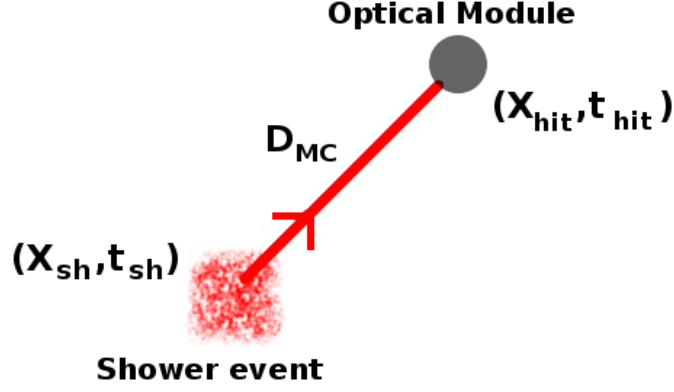


Figure 18: Distance  $D_{MC}$  between a shower interaction vertex with space-time position of  $(X_{sh}, t_{sh})$  and a hit Optical Module with space-time position  $(X_{hit}, t_{hit})$ .

As expected, the probability density functions of both simulations are distributed around zero. The AMHiC simulation is peaking a bit higher than the standard Antares simulations. This effect is expected, since CC showers deposit more light compared to NC showers. Figure 17 is not comparing the two simulation tools, since two different types of interactions (CC and NC) have been simulated. Therefore, this result indicates that the AMHiC tool works well for the Antares geometry. In the next subsection, the application of AMHiC is shown for the KM3NeT detector geometry.

## 6.2 Simulation of showers in KM3NeT with aAMHiC and AGeMOM

Showers can be simulated in KM3NeT with two tools: AMHiC and AGeMOM. AMHiC had to be adjusted for simulations in KM3NeT, by implementing a simplified geometry of KM3NeT. The tower-structure (Section 3.1) of KM3NeT, with Detection Units on a minimal separation of 130 meters was used, but with the modification that the PMTs of a multi-PMT Optical Module are treated as 31 clustered Optical Modules. Also parameters as Can size and detector depth had to be adjusted and the very important KM3NeT Photontables, consisting of specifications of photons traveling through seawater, had to be implemented. The newly developed tool is called aAMHiC (adjusted Anis Mmc Hit Constructor). Showers in KM3NeT can be produced using the current AGeMOM tool by generating CC  $\nu_e$ -induced hadronic showers. The results of simulations for  $\nu_e$ -induced hadronic showers in KM3NeT with the aAMHiC and AGeMOM simulation tools are presented in Figure 19, where the probability density functions for  $\Delta t(\text{true})$  (as defined in Section 6.1) are shown.

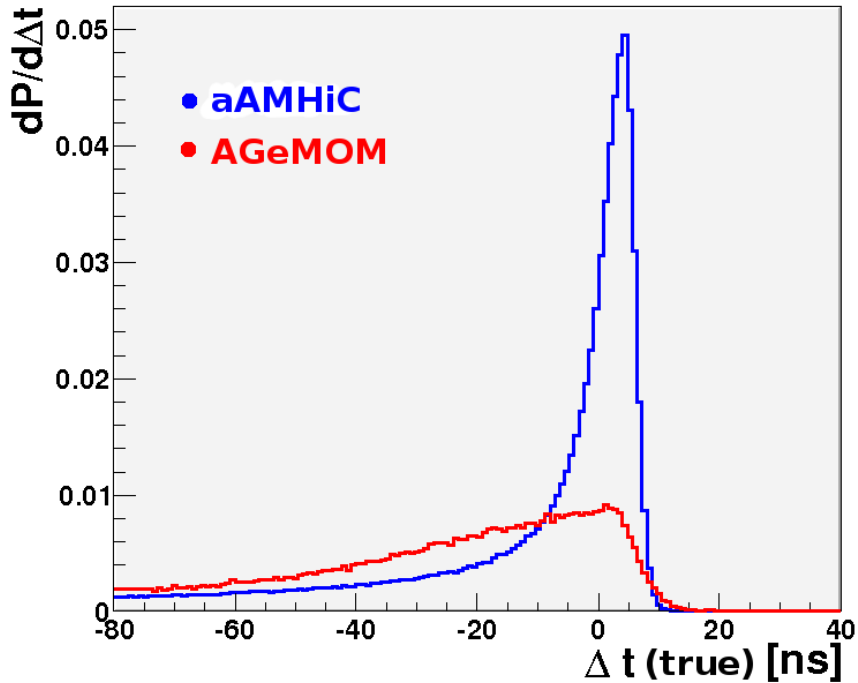


Figure 19: *Probability density functions of the aAMHiC (blue) and AGeMOM (red) simulation tools for  $\nu_e$ -induced electromagnetic + hadronic showers in KM3NeT.*

The AGeMOM simulation tool results in a very broad distribution<sup>1</sup>, while the aAMHiC tool shows a sharp peak around zero seconds. Therefore, the aAMHiC simulation tool is preferred above the AGeMOM tool.

<sup>1</sup>In a discussion with Qader Dorosti, it appeared that the light of the particles is distributed randomly in all directions with AGeMOM.

### 6.3 Reconstruction of showers in KM3NeT

Although aAMHiC is the preferred simulation tool, the reconstruction of showers has been done using both the aAMHiC and the AGeMOM simulation tools for comparison.

The results for shower reconstruction with the new selection strategy after the AGeMOM simulation are shown in Figure 20. The peak of the time difference distribution (Figure 20 b) is shifted to around -15 ns and the shower interaction vertex (Figure 20 a) to around 30 meters away from the Monte Carlo position. The reconstructed showers show a systematical shift in space-time position. The shift of the time distribution will be pointed out below. The cause of the unexpected shift of the distribution of the position is not fully understood. Possibly the shift is caused by the large distance between the Optical Modules in a bar. Further investigations must be done to resolve this problem.

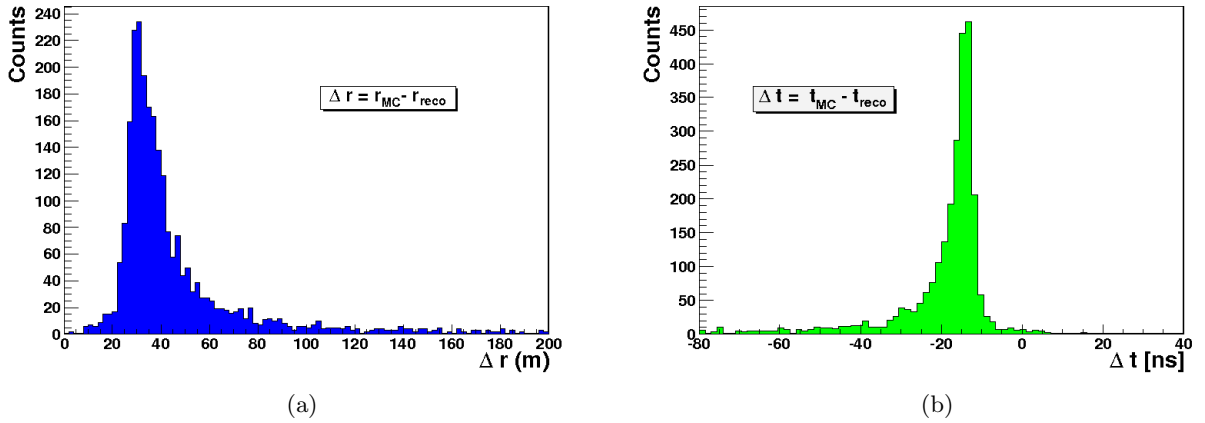


Figure 20: *Reconstruction of electromagnetic showers after the AGeMOM simulation: (a) distance of reconstructed shower from true position, (b) timing of reconstructed shower.*

The results of shower reconstruction with the new selection strategy after the aAMHiC simulation are shown in Figure 21. The statistics is not very high as it takes time in the order of days to generate 800 shower events. After the reconstruction has been applied, only 45 events remain. The difference in the shower interaction vertex (Figure 21 a) is distributed around zero and the time difference distribution (Figure 21 b) peaks as well at -15 ns with a shift of the edge value by about -8 ns.

Possibly, the shift is due to the shower development, i.e. shower particles travel a few meters with less than the speed of light, projecting the shower not exactly as a point-source of light. If we assume that these showers have a length of 10 meters and the interaction vertex is reconstructed in the centre (the shower centre of gravity), i.e. 5 meters from the starting point of the shower, then the time difference ( $\Delta_{vertex}$ ) of the true MC starting point and the reconstructed vertex is (roughly):

$$\Delta t = \frac{\Delta_{vertex}}{v_{light}} = \frac{5 \text{ m}}{3 * 10^8 \text{ m/s}} = 16 \text{ ns}. \quad (18)$$

This shift roughly corresponds to the peak value of the distribution. The tail on the left side of the peak can be caused through the radiation of many electrons ( $e^-$ ) and positrons ( $e^+$ ) in the late stage of the shower. The reconstruction after the aAMHiC simulation results in a much better precision in determining the position of the shower interaction vertex in KM3NeT than the reconstruction after the

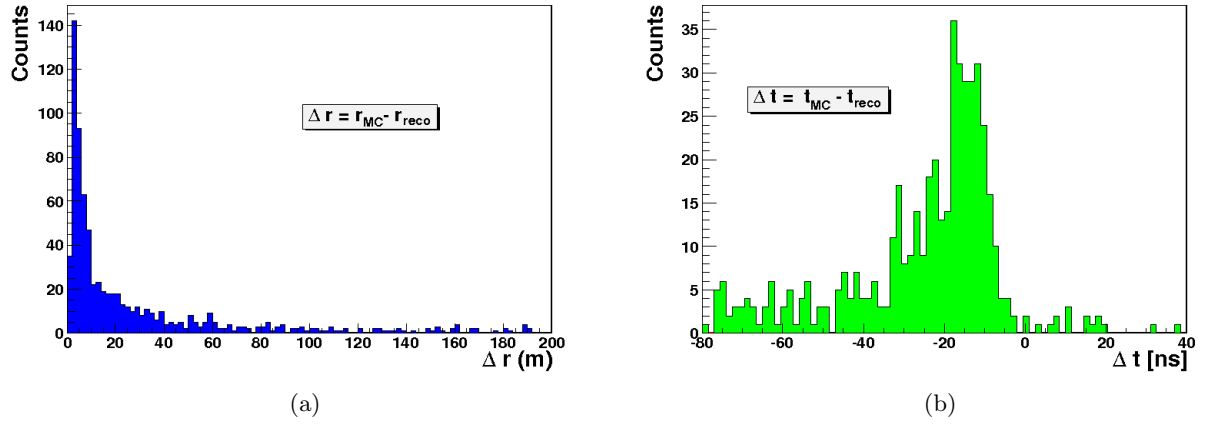


Figure 21: *Reconstruction of electromagnetic showers after the aAMHiC simulation: (a) distance of reconstructed shower from true position, (b) timing of reconstructed shower.*

AGeMOM simulation. Therefore, reconstruction and shower selection will be applied on the aAMHiC simulations.



## 6.4 M-estimator performance and cut in KM3NeT

The M-estimator and Residual output values, as defined in Section 5, are evaluated as reconstruction quality parameters. Lower values for the reconstruction quality parameters are expected for a shower-like event, compared to those for muon tracks. The probability densities of the M-estimator values of electromagnetic showers and  $\nu_\mu$ -induced muons, both simulated with aAMHiC, are shown in Figure 22. A large part of the muons will be rejected if a cut is applied after the peak of the electromagnetic showers.

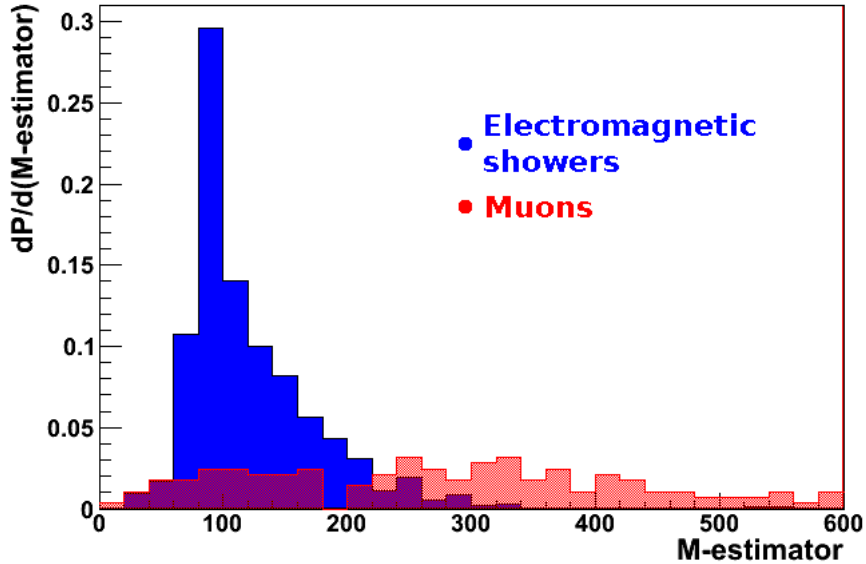


Figure 22: Probability density of the M-estimator for electromagnetic showers (blue) and muons (red), both simulated with aAMHiC.

In addition, a similar cut can be applied for the Residual quality parameter. To show how showers can be distinguished from muons in KM3NeT, the Residual parameter is plotted against the M-estimator in Figure 23 for electromagnetic showers and  $\nu_\mu$ -induced muons simulated with aAMHiC. A majority of the reconstructed electromagnetic shower events can be found in the lower-left corner. The majority of the reconstructed muons have large Residual and M-estimator values. A cut can be made e.g. at Residual 200 and M-estimator 200 in order to (most likely) select shower events and therefore obtain high purity. Typical values for reconstruction of simulations in Antares, done by [38], are 20% efficiency and a purity higher than 90%.

The high M-estimator values, in comparison to those in Figure 16, for electromagnetic showers simulated with the aAMHiC tool could be caused by the representation of the 31 3-inch PMTs of an Optical Module in KM3NeT as 31 clustered (small) Optical Modules. The problem may be caused by the photon tables produced by Photonics (Section 4.3). The used parametrizations are done for the PMTs in Antares and need to be re-parametrized with KM3NeT PMT specifications. Development on the parametrizations for KM3NeT is in progress. Implementing the results of this new parametrization may lead to reconstructed showers with lower M-estimator values. Optimization of the quality cuts then result in the selection of more showers with less muons. Hence, the purity of the selection strategy will increase.

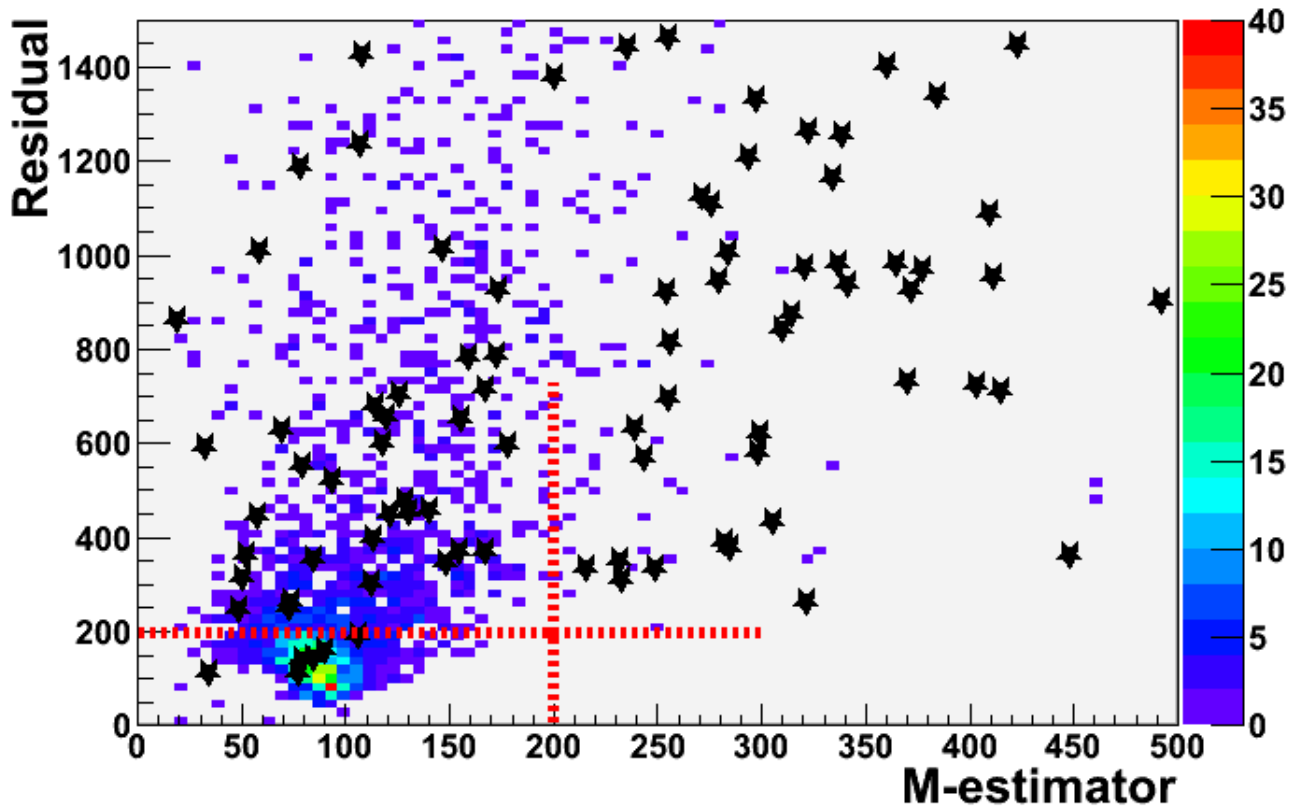


Figure 23: *Residual versus M-estimator parameters for muon tracks (denoted by black stars) and electromagnetic showers (density colors), simulated in KM3NeT with aAMHiC. A possible cut at Residual 200 and M-estimator 200 is denoted with dashed red lines.*

## 7 Summary

To study the origin of Cosmic Rays, a new large-volume neutrino telescope (KM3NeT) will be built. Neutrinos can be detected through their interactions with matter, creating relativistic secondary particles. In water, these secondary particles will emit Cherenkov light, which can be measured by KM3NeT through detection lines with Multi-PMT Optical Modules. Initially, KM3NeT has been designed to detect muon tracks, but in this work the extension of KM3NeT for showers has been demonstrated.

The performance of KM3NeT and Antares has been tested by simulating  $\nu_e$ -induced hadronic showers and  $\nu_\mu$ -induced hadronic showers using AMHiC and AGeMOM simulating tools. The AMHiC simulating tool has been compared to a standard tool for Antares simulations and was found to be working well for Antares. Thereafter, AMHiC had been adjusted to aAMHiC for simulations in KM3NeT. In parallel, simulations in KM3NeT have been done with the existing AGeMOM tool. The aAMHiC tool was found to give the best results, as its simulations gave the best accuracy in determining the space-time coordinates of the shower interaction vertex. As the last step, a new reconstruction strategy had been applied on simulations of  $\nu_e$ -induced hadronic showers and  $\nu_\mu$ -induced muons.

With the ability to reconstruct showers, the next challenge was to distinguish the showers from the huge atmospheric muon background. A quality cut, developed for Antares, can be applied in order to distinguish shower events from muons. This has been demonstrated for simulations with aAMHiC, showing that this newly developed tool can be used for shower selection in KM3NeT.

The simulation methods aAMHiC and AGeMOM have produced showers in KM3NeT which can be reconstructed with a new selection strategy in order to distinguish shower events from muons with high efficiency and purity.

## References

- [1] D.J. Bird et al., "*Detection of a Cosmic Ray with Measured Energy Well Beyond the Expected Spectral Cutoff due to Cosmic Microwave Radiation*", arXiv:astro-ph/9410067v1
- [2] M. Drees, "*The Top-Down Interpretation of Ultra-High Energy Cosmic Rays*", J. Phys. Soc. Jpn. 77 (2008) Suppl. B, 1618
- [3] G. Sigl, "*Ultrahigh-Energy Cosmic Rays: Physics and Astrophysics at Extreme Energies*", Science 291 (5501) (2001) 73-79
- [4] [http : //www.auger.org/observatory/](http://www.auger.org/observatory/)
- [5] [http : //fermi.gsfc.nasa.gov/science/overview.html](http://fermi.gsfc.nasa.gov/science/overview.html)
- [6] [http : //www.mpi-hd.mpg.de/hfm/HESS/pages/about/](http://www.mpi-hd.mpg.de/hfm/HESS/pages/about/)
- [7] [http : //antares.in2p3.fr/Overview/index.html](http://antares.in2p3.fr/Overview/index.html)
- [8] [http : //icecube.wisc.edu/about/explained](http://icecube.wisc.edu/about/explained)
- [9] [http : //km3net.org/flyer/KM3NeT-publicity-sheet-may2007-new-banner.pdf](http://km3net.org/flyer/KM3NeT-publicity-sheet-may2007-new-banner.pdf)
- [10] A. Finkbeiner, "*Looking for Neutrinos, Nature's Ghost Particles*", Smithsonian magazine, November 2010
- [11] R. Nave, "*Fermi Theory of Beta Decay*", [http : //hyperphysics.phy-astr.gsu.edu/hbasequantum/fermi2.html](http://hyperphysics.phy-astr.gsu.edu/hbasequantum/fermi2.html)
- [12] C.L. Cowan, F. Reines, F.B. Harrison, H.W. Kruse, A.D. McGuire, "*Detection of the Free Neutrino: A Confirmation*", Science, 124 (3212) (1956) 103-104
- [13] Brookhaven National Laboratory, "*Discovery of the Muon-Neutrino*", [http : //www.bnl.gov/bnlweb/history/nobel/nobel88.asp](http://www.bnl.gov/bnlweb/history/nobel/nobel88.asp)
- [14] Fermilab, "*Physicists Find First Direct Evidence for Tau Neutrino at Fermilab*", 20 july 2000, [http : //www.fnal.gov/pub/presspass/press\\_releases/donut.html](http://www.fnal.gov/pub/presspass/press_releases/donut.html)
- [15] OPERA Collaboration, "*Measurement of the neutrino velocity with the OPERA detector in the CNGS beam*", arXiv:1109.4897v1
- [16] A.J. Heijboer, "*Track Reconstruction and Point Sources Searches with ANTARES*", PhD Thesis, Amsterdam, 2004, ISBN 90-6464-510-8
- [17] E. Waxman, "*Cosmological gamma-ray bursts and the highest energy cosmic rays*", Phys. Rev. Lett. 75 (1997) 386-389, [http : //arxiv.org/abs/astro-ph/9505082](http://arxiv.org/abs/astro-ph/9505082)
- [18] E. Waxman, J.N. Bahcall, "*High energy neutrinos from cosmological gamma-ray burst fireballs*", Phys. Rev. Lett. 78 (1997) 2292-2295, [http : //arxiv.org/abs/astro-ph/9701231](http://arxiv.org/abs/astro-ph/9701231)
- [19] A. Levinson, E. Waxman, "*Probing Micro-quasars with TeV neutrinos*", Phys. Rev. Lett. 87 (2001) 171101, [http : //arxiv.org/abs/hep-ph/0106102](http://arxiv.org/abs/hep-ph/0106102)

- [20] Z. Xing, S. Zhou, "*The Glashow resonance as a discriminator of UHE cosmic neutrinos originating from  $p\gamma$  and  $pp$  collisions*", arXiv:1105.4114v4
- [21] P. Mehtaa, W. Winter, "*Interplay of energy dependent astrophysical neutrino flavor ratios and new physics effects*", arXiv:1101.2673v2
- [22] P.A. Cherenkov, "*Visible radiation produced by electrons moving in a medium with velocities exceeding that of light*", Phys. Rev. 52 (4) (1937) 378-379
- [23] B. Hartmann, "*Reconstruction of Neutrino-Induced Hadronic and Electromagnetic Showers with the ANTARES Experiment*", PhD Thesis, Erlangen 2006, arXiv:astro-ph/0606697v1
- [24] KM3NeT Technical Design Report, ISBN 978-90-6488-033-9 2010,  
[http : //km3net.org/KM3NeT – TDR](http://km3net.org/KM3NeT-TDR)
- [25] "*Technical description of the PPM of the KM3NeT detection unit*",  
[http : //km3net.org/PPM/KM3NeT\\_FL\\_REP\\_PPM – description.pdf](http://km3net.org/PPM/KM3NeT_FL_REP_PPM-description.pdf)
- [26] N. Hobgood, [http : //en.wikipedia.org/wiki/Pyrosome](http://en.wikipedia.org/wiki/Pyrosome)
- [27] T.R. DeYoung, "*IceTray: a Software Framework for IceCube*", International Conference on Computing in High Energy Physics and Nuclear Physics, Interlaken 2004
- [28] [http : //sales.hamamatsu.com/  
en/products/electron – tube – division/detectors/photomultiplier – tubes/part – r6233 – 100.php](http://sales.hamamatsu.com/en/products/electron-tube-division/detectors/photomultiplier-tubes/part-r6233-100.php)
- [29] ET Enterprises, D783FLA preliminary data sheet, 19 may 2011
- [30] [http : //www.nestor.noa.gr/](http://www.nestor.noa.gr/)
- [31] [http : //nemoweb.lns.infn.it/index.php?id = 94&subid = 185](http://nemoweb.lns.infn.it/index.php?id=94&subid=185)
- [32] A. Gazizov, M.P. Kowalski, "*ANIS: High energy neutrino generator for neutrino telescopes*", Comput. Phys. Commun. 172 (2005) 203
- [33] D. Chirkin, W. Rhode, "*Propagating leptons through matter with Muon Monte Carlo (MMC)*", arXiv:hep-ph/0407075v2
- [34] E. Presani, "*Simulation in SeaTray: a guide for the KM3NeT/ANTARES user*", ANTARES Internal Note, 2010
- [35] C. Kopper, "*Performance Studies for the KM3NeT Neutrino Telescope*", PhD Thesis, Friedrich-Alexander-Universität Erlangen-Nürnberg, 2010
- [36] Geant4 Collaboration, "*Geant4a simulation toolkit*", Nuclear Instruments and Methods in Physics Research Section A: Accelerators, Spectrometers, Detectors and Associated Equipment Volume 506, Issue 3, 1 July 2003, Pages 250-303
- [37] Z. Zhang, "*Parameter estimation techniques: A tutorial with applications to conic fitting*", Image and Vision Computing Journal 15 (1997) 59
- [38] Q. Dorosti, "*Neutrino-induced showers in the ANTARES Deep-Sea Telescope*", Contribution to VLVnT 2011, to be published

- [39] E. Presani, C.J. Reed, "*Shower reconstruction in ANTARES: an M-estimator fit algorithm*",  
NIKHEF Amsterdam, 3 November 2010

## Appendix A

Script used to propagate showers. From [35].

```
from I3Tray import *
* Load libraries
load("libicetray")
load("libinterfaces")
load("libdataclasses")
load("libphys-services")
load("libsimclasses")
load("libsim-services")
load("libdataio")
load("libg4sim-interface")
load("libmuon-sim")
load("libicepick")

* Instantiate a tray
tray = I3Tray()
if useBunches:
    tray.AddService("I3SPRNGRandomServiceFactory", "sprngrandom",
        NStreams = 1000000,
        Seed = rngSeed,
        StreamNum = options.BUNCHNUM)
    *outstatefile = simDir + "/g4sim/work_E-%i/%i/rng_Bunch%06d.state" % (gammaIndex, runNumber)
else:
    tray.AddService("I3SPRNGRandomServiceFactory", "sprngrandom",
        NStreams = 2,
        Seed = rngSeed,
        StreamNum = 1)

tray.AddService("I3ReaderServiceFactory", "PhysicsReader",
    FileNameList = inputfilesWithGCD)

Data is combined and stored in frames (Section 4) with the "Muxer".

tray.AddModule("I3Muxer", "muxer")

if useBunches:
    tray.AddModule("I3IcePickModule<I3SkipNEventFilter>", "select_one_frame_only",
        DiscardEvents = True,
        SkipNevents = (options.BUNCHNUM-1)*options.BUNCHSIZE,
        NEventsToPick = options.BUNCHSIZE)

tray.AddModule("Copy", "save_original_cmc_tree",
    Keys = ["I3MCTree", "I3MCTreeBeforeG4Sim"])
```

Rules for propagation are given in the module below. The energy threshold for the propagation of secondary particles and the size of The Can (Section 4.1) are entered here. Also one can choose to propagate only muons or propagate only electrons and positrons as secondaries.

```
tray.AddModule("I3G4SimInterface","sim-interface",
    MCTreeName = "I3MCTree",
    DirectionalMCHitMapName = "G4SimHits",
    SecondaryProductionCutoffEnergy = 0.5*I3Units.GeV,
    AdditionalCanSize = 300.*I3Units.m,
    OnlyElectronsAndPositronsAsSecondaries = False,
    TreatScatteredPhotonsAsAbsorbed = False,
    MMCPrePropMode = True,
    MMCTrackListName = "MMCTrackList",
    PropagateMuonsOnly = False,
    DisablePhotonOutput = True,
    RandomSeed = MMCseed)
```

In the "Interface" module the output of photons is disabled. Photons are produced through the module below. Photontables consist of specifications of photons traveling through water.

```
tray.AddModule("I3MuonSimulator", "muon-sim",
    MCTreeName = "I3MCTree",
    DirectionalMCHitMapName = "G4SimHits",
    AddHitsToExistingHitMap = False,
    PhotonDataFilenameMuon = photonTableFileMuon,
    PhotonDataFilenameShower = photonTableFileShower,
    TreatScatteredPhotonsAsAbsorbed = False)

if scratchDir:
    useOutfileName = scratchDir + outfile
else:
    useOutfileName = outdir + outfile
if useBunches:
    tray.AddModule("I3Writer", "writer",
streams = ["Physics"],
filename = useOutfileName)
else: # write full GCD if we do not use bunches
    tray.AddModule("I3Writer", "writer",
filename = useOutfileName)

tray.AddModule("TrashCan","trashcan")

# Execute the Tray
tray.Execute()
tray.Finish()
```



## Appendix B

Scripts for simulation and M-estimator evaluation can be found on the IN2P3 computing center at Lyon (<http://cc.in2p3.fr/>). The files are spread over three sub folders:

`/shower-sim`, `/muon-sim` and `/shower-reco`,

placed in:

`/sps/km3net/users/loehner/seatray/build/`

Simulations in Antares with AMHiC are done with:

`/shower-sim/resources/scripts/gerrit-test-Elecshower.py`

Simulations in KM3NeT with aAMHiC are done with:

`/shower-sim/resources/scripts/KM3NetProduction.py`

Simulation in KM3NeT with AGeMOM are done with:

`/muon-sim/resources/scripts/batchNeutrinoGen.py`

for particle generation,

`/muon-sim/resources/scripts/batchSimG4sim.py`

for particle propagation, and

`/muon-sim/resources/scripts/batchSimMultiOMs_addition.py`

for hit construction on multi-PMT Optical Modules. The requested muon and shower tables can be found in:

`/sps/km3net/users/kopper/tables/`

The M-estimator, which has to be applied after the simulations, can be found in:

`/shower-reco/resources/scripts/gerrit-Mestimator.py`

for Antares simulations and

`/shower-reco/resources/scripts/gerrit-KM3NET-Mestimator.py`

for KM3NeT simulations. The M-estimator script produces a text file with columns, corresponding to 6 parameters. These parameters are:

`mes` (M-estimator), `res` (Residual), `delta_r`, `delta_t`, `chrge` (charge) and `energy`.

The parameters can be evaluated using

`shower-reco/results/analysis/gerrit-analysis/analysis.C`

